Heliyon 9 (2023) e13679

Contents lists available at ScienceDirect

Heliyon

journal homepage: www.cell.com/heliyon

Research article

Fabrication and wear behaviour of Mg-3wt.%Al-*x* wt. % SiC composites

S. Jayasathyakawin, M. Ravichandran [*]

Department of Mechanical Engineering, K. Ramakrishnan College of Engineering, Samayapuram, Trichy, 621112, India

A R T I C L E I N F O

Keywords:
Magnesium
Silicon carbide
Composite
Wear
Powder metallurgy
Taguchi

A B S T R A C T

In this work, Silicon Carbide (SiC) reinforced Mg/3Al matrix composite was developed via powder metallurgy (PM) method. Friction coefficient (COF) and wear rate (WR) of the composite was studied using Pin on disc wear tester. Scanning Electron Microscope (SEM) was used to investigate the microstructure of sintered samples. During the experiments, L16 orthogonal design was followed. Wear analysis was done with four wear control factors such as the reinforcement (Wt.%), the applied load ('P'), the sliding velocity ('V') and the sliding distance ('D'). In this study, the optimal combination of parameters was found using signal-to-noise (S/N) ratio analysis. Based on the analysis of variance (ANOVA), the 'P' and Wt.% of SiC are the two parameters that have the greatest influence on WR and COF. From the analysis, Mg/3Al/9SiC-composites exhibited better wear properties among other composition tested. Worn surface analysis was conducted for the tested samples and the SEM images are reported.

1. Introduction

Metal matrix composites (MMCs) are strengthened with fibers, whiskers, and particulates. MMCs are manufactured with liquid phase sintering, stir casting and powder metallurgy [1]. Mg alloys offer little handling flexibility, in contrast, Mg composites are extremely lightweight and offer huge advantages, such as high elasticity, high strength and resistance to creep and wear [2]. Mg matrix composites, apart from their strength and elasticity, are high resistant to wear, which makes them an excellent choice for automotive, aerospace and military applications. The properties of the MMCs have been affected by matrix, reinforcement particles, particle shapes, particle sizes and uniform distribution of reinforcements [3]. Mg is an excellent material for manufacturing because of its low weight. In terms of mineral abundance, Mg is the eighth most abundant element on Earth [4]. Aluminium, Titanium, Mg and alloys are low-density metals used as matrix materials [5].

SiC has been used as excellent reinforcement materials for Mg based composite materials. SiC is resistant to heat, strong, thermal shock-resistant and has a high modulus of elasticity [6]. By reinforcing SiC with Mg matrix, tribological properties and corrosion resistance are improved with lower energy consumption [7]. Research has been conducted on the tribological behavior of SiC incorporated Mg based composites [8]. The properties of Mg and its alloys are improved when SiC particles are incorporated, including strength, density, solidity and wear resistance [9]. SiC particles develop good microstructure in Mg based composite materials. By increasing the SiC particles, one can produce composites with higher strength [5,10,11].

PM produces shapes that are similar to or equal to predictable shapes and as much as possible, should not require metal removal

* Corresponding author.
E-mail address: smravichandran@hotmail.com (M. Ravichandran).

https://doi.org/10.1016/j.heliyon.2023.e13679
Received 2 November 2022; Received in revised form 8 February 2023; Accepted 8 February 2023
Available online 12 February 2023
2405-8440/© 2023 The Authors. Published by Elsevier Ltd. This is an open access article under the CC BY-NC-ND license (http://creativecommons.org/licenses/by-nc-nd/4.0/).

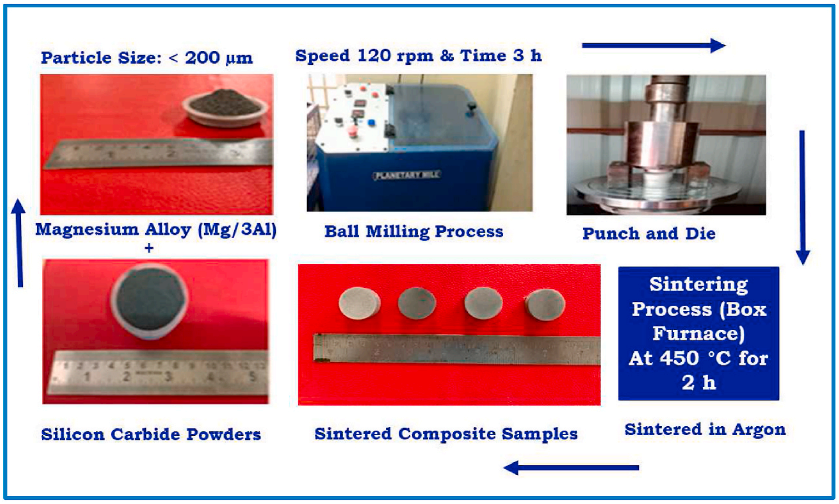

Fig. 1. Materials and experimental setup.

from the powder. A new study has found that SiC particles exhibit optimal mechanical properties and minimal micro-porosity as a result of their necklace-like circulation in metal matrix [12]. By combining calcium-based ceramics with Mg implants, corrosion rates are reduced but corrosion occurs uniformly within the cell due to uniform corrosion attacks. PM is a promising method for reducing corrosion rates [13]. Fine powdered catalysts, compression and controlled heating under controlled conditions could be used to bond powdered materials. PM can be used to manufacture most metallic alloys and composites with required dimensions and good microstructure [14,15].

García Rodríguez et al. demonstrated the wear performance of magnesium alloy and AZ91/SiC composites added with various percentage of SiC particles under normal loads and sliding speeds using pin-on-disc configuration [30]. Hu Yong et al. investigated the wear performance of Mg composites with Mg_2Si and reported that the impact of Si, 'P' and 'D' on the wear performance of Mg composites [31]. Jojith et al. studied the aluminium composites incorporated with wt. % (0, 4, 8 & 12) of B_4C particles and found that varying 'P', 'V', 'D' and Wt. % would affect the tribological performance of the composites [16]. Alagarsamy et al. demonstrated that the Design of Experiments (DOE), Taguchi method is a well-known procedure for evaluating control parameter effects on responses and they evaluated the effects of wear on MMCs [17].

Dharmalingam et al. studied the wear behaviour of AA-15% SiC as well as AA-15%SiC-3% Gr composites by Taguchi DOE [18]. Altinkok et al. summarized the wear performances of Alumina and SiC reinforced aluminium-based hybrid composites and obtained a important enhancement in wear resistance [24]. Ravindran et al. focused on the wear behavior of a hybrid aluminium alloy composites contain SiC and Gr particles process by PM and they examined the various parameters using ANOVA to determine the impact on WR and COF [25]. Suresha and Sridhara investigated the aluminium composites reinforced with SiC & Gr particles and observed that the wear resistance of hybrid composites was higher than that of aluminium–SiC composites [26]. Rao et al. examined the wear of AA7075/TiC composites and described that, the decreased TiC content increased the wear loss [27]. Baskaran et al. reported that, DOE is a influential tool and it is employed to optimize design, select parameters, control processes, and predict product performance characteristics [28]. Dhanalakshmi et al. implemented the Taguchi design to determine the wear parameters for Al7075–Al_2O_3/B_4C MMCs. They reported the relationship between the wear parameters against WR and COF [29].

Moslem Tayyebi et al. reported that COF and Wear Rate was reduced for Al/Cu functionally graded composite while increasing the reinforcement particles [32]. Pham Van Trinh et al. demonstrated that, the COF and specific WR of the hybrid composites were reduced by the addition of CNTs. However, the wear rare is increased for the increase in 'P' even though the CNT content is increased [33]. Many researchers reported that the coating of reinforcement particles also improved wear resistance [34]. Junliu Ye et al. investigated the effect of Ti in AZ31 matrix composites through stir casting process and reported that Ti particles can successfully decrease the COF of Ti-AZ31 composites during sliding [35]. Jatinder Kumar et al. reported that, significant reduction in WR is possible when the reinforcement particulates introduced in the base ductile alloy. A little fall in the COF is observed when SiC particulates are added in the Al–SiC–Cr matrix [36]. The addition of SiC particles to the Al matrix increased the hardness of the composite, while it reduced both the WR and COF due to the better distribution of SiC particles and their higher hardness [37].

Form the above literatures, the aim of the present work is to investigate the WR and COF of Mg/3Al/3/SiC, Mg/3Al/6SiC and Mg/3Al/9SiC composites. Pin-on-disc apparatus was employed to conduct the test, with various control wear parameters. By using the Taguchi technique, we analyzed the effect of wear parameters on WR and COF. SEM was used to analyse the worn surface of the proposed composite samples.

2. Experimental procedure

In this work, Mg/3Al alloy and composites such as, Mg/3Al/3SiC, Mg/3Al/6SiC and Mg/3Al/9SiC were produced using PM route.

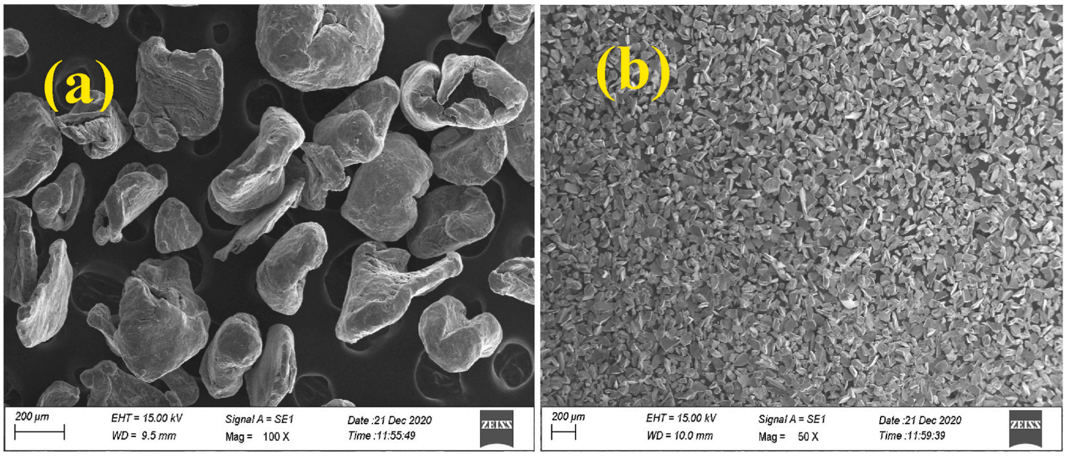

Fig. 2. SEM image (a) Mg (b) SiC.

Table 1
Parameters and levels.

Wt. % SiC	0	3	6	9
'P' (N)	5	10	15	20
'D' (m)	500	1000	1500	2000
'V' (m/s)	1	2	3	4

Table 2
Experimental details.

Exp. Number	Wt. % of SiC	'P' (N)	'D' (m)	'V' (m/s)	Wear rate × 10^{-3} mm^3/m	COF	S/N Ratio (WR)	Mean (WR)	S/N (COF)	Mean (COF)
1	0	5	500	1	7.1135	0.49	−17.0417	7.1135	6.196078	0.49
2	0	10	1000	2	8.834	0.55	−18.9231	8.834	5.192746	0.55
3	0	15	1500	3	11.3524	0.61	−21.1018	11.3524	4.293403	0.61
4	0	20	2000	4	13.6234	0.64	−22.6857	13.6234	3.876401	0.64
5	3	5	1500	2	9.2493	0.42	−19.3222	9.2493	7.535014	0.42
6	3	10	2000	1	9.5449	0.44	−19.5954	9.5449	7.130946	0.44
7	3	15	500	4	8.7531	0.59	−18.8432	8.7531	4.58296	0.59
8	3	20	1000	3	10.638	0.62	−20.5372	10.638	4.152166	0.62
9	6	5	2000	3	7.2535	0.43	−17.211	7.2535	7.330631	0.43
10	6	10	1500	4	6.3439	0.48	−16.0471	6.3439	6.375175	0.48
11	6	15	1000	1	7.8638	0.56	−17.9126	7.8638	5.036239	0.56
12	6	20	500	2	8.1432	0.65	−18.2159	8.1432	3.741733	0.65
13	9	5	1000	4	3.2457	0.35	−10.2262	3.2457	9.118639	0.35
14	9	10	500	3	3.9782	0.39	−11.9937	3.9782	8.178708	0.39
15	9	15	2000	2	4.195	0.43	−12.4546	4.195	7.330631	0.43
16	9	20	1500	1	5.485	0.52	−14.7835	5.485	5.679933	0.52

Fig. 1 shows the experimental procedure followed in this work. Mg, Al and SiC powders were procured from Kemphasol in Mumbai, India. Fig. 2(a) and (b) show the SEM image of Mg and SiC.

The powders were blended in high energy ball mill at a speed of 120 rpm for 3 h, with 10:1 ball to powder ratio. The milled powders were compacted in a hydraulic press (Model: Universal Tun-400) with the uniform load for all the samples. Zinc stearate was applied as lubricant during ejecting the compact. Sintering of the green compacts was done in a controlled Argon furnace (Model: Box furnace 1200 °C) at 450 °C in 10°/min increments for 2 h. Furnace cooling was done for the sintered samples. SEM (Make: TESCAN VEGA3-Wsource) was used to analyse the microstructure of the produced samples. In order to observe the microstructure of the samples, standard mechanical polishing techniques were followed.

To study the dry sliding wear behaviour of the proposed Mg/3Al/SiC composite material, the wear pins were made at 10 mm dia and 30 mm height. The compositions of the composites are Mg/3Al/3SiC, Mg/3Al/6SiC and Mg/3Al/9SiC. ASTM G99 standard was used to conduct the wear test. The EN 31 Hardened steel disc has a diameter and thickness of 165 mm and 8 mm, respectively were used as disc object. A weighing balance with a accuracy of 0.00001 g was used. Tables 1 and 2 illustrates the control factors, their levels, and the experimental conditions for wear test. On the pin-on-disc apparatus (Make: Ducom Wear test), load cells measure

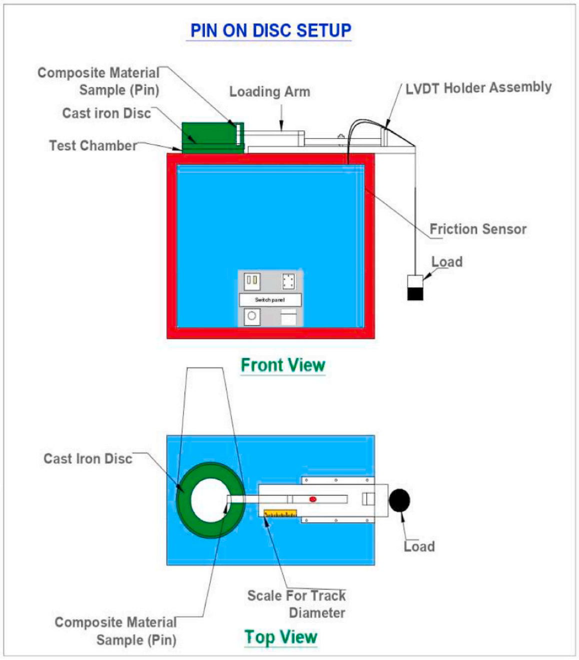

Fig. 3. Schematic of pin on disc.

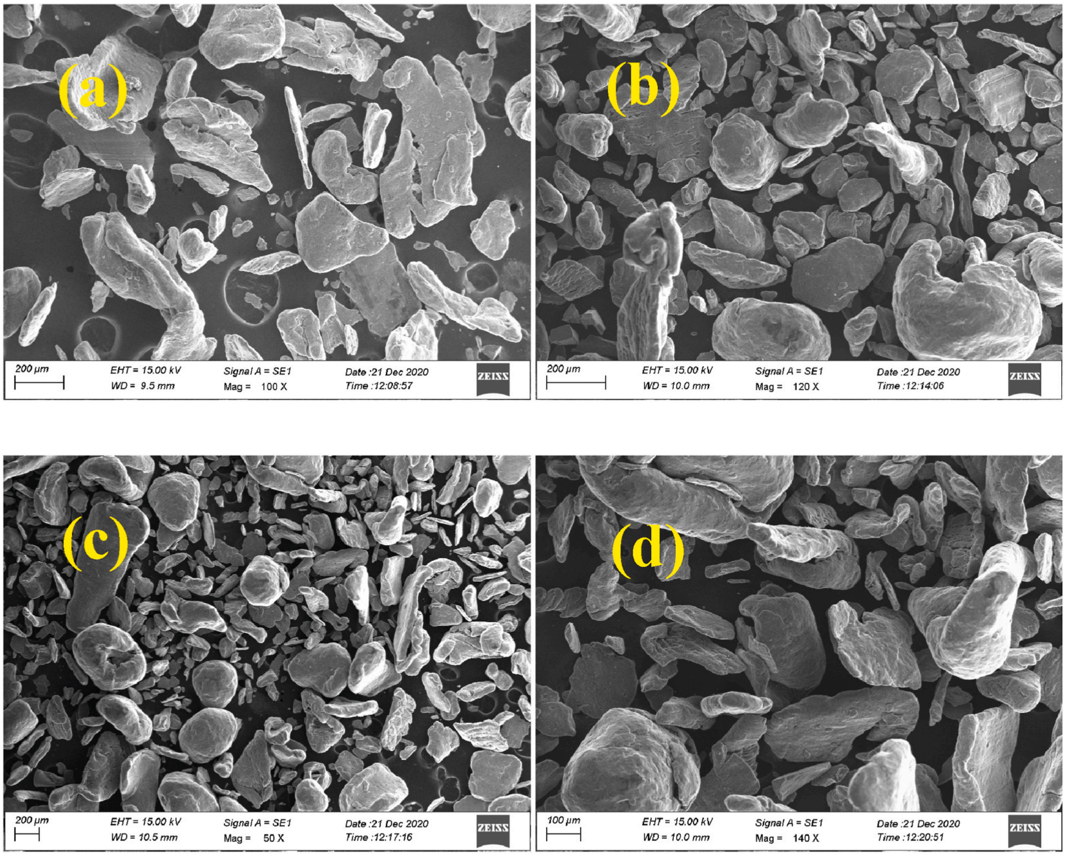

Fig. 4. SEM images of ball milled (a) Mg/3Al/3SiC (b) Mg/3Al/6SiC (c) & (d) Mg/3Al/9SiC powders.

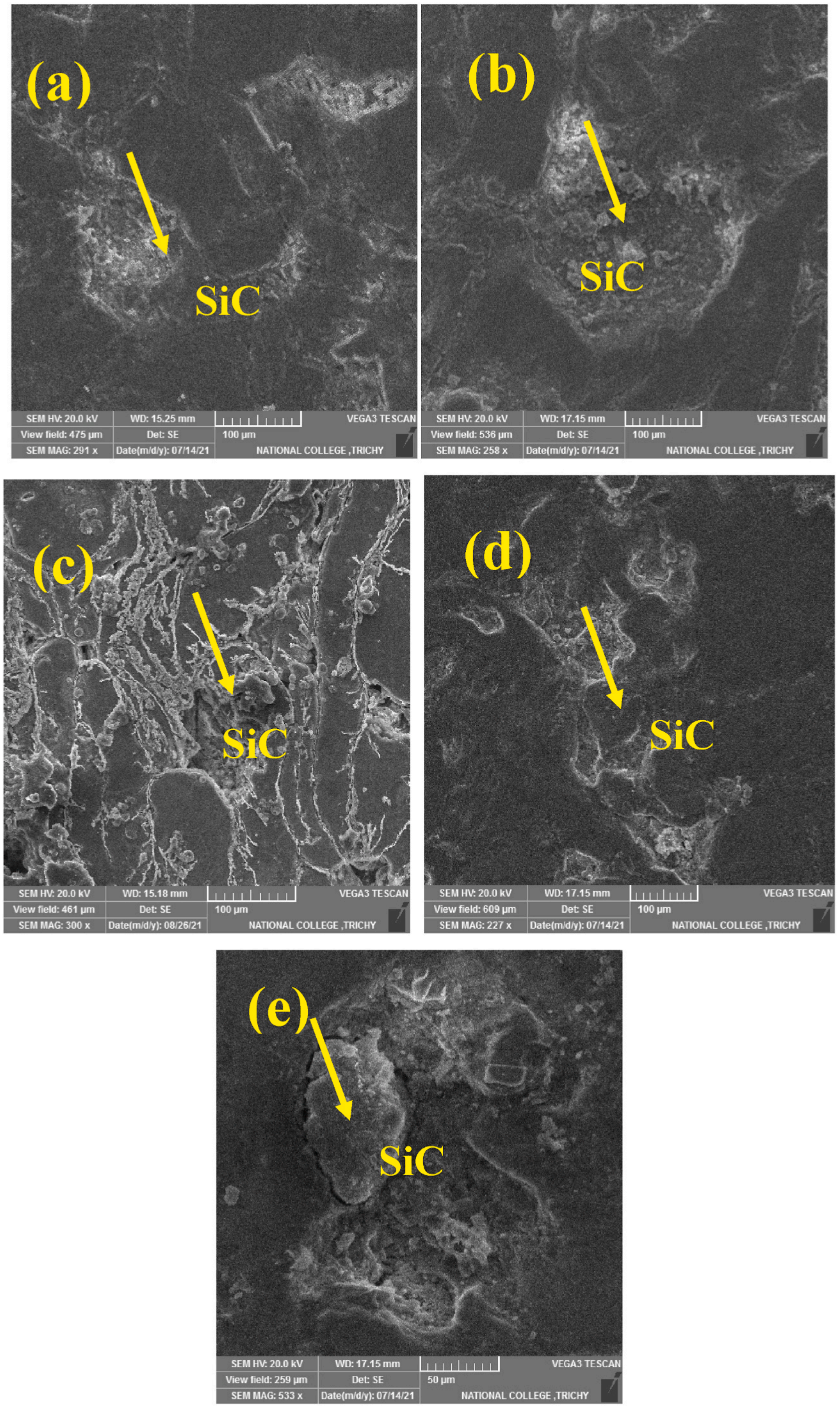

Fig. 5. SEM images of Sintered composites (a) Mg/3Al/3SiC, (b) Mg3Al/6 SiC, (c) Mg3Al/9SiC, (d) and (e) Mg3Al/9 SiC.

tangential forces on specimens. Fig. 3 displays the schematic of Pin on disc setup. According to the wear data obtained for the specimens, the WR and COF are calculated [18]. This study consisted four control factors with four levels. The objective was to optimize wear parameters to achieve minimum wear rate [19]. The WR was calculated as equations (1) and (2).

$$WR = \text{Mass loss} \times \text{Density}/D \ (mm^3/m) \quad (1)$$

$$V = \Pi \ D \ N/1000 \quad (2)$$

Table 3
S/N ratios for WR.

Level	Wt.% of SiC	'P' (N)	'V' (m/s)	'D' (m)
1	−19.94	−15.95	−17.33	−16.52
2	−19.57	−16.64	−17.23	−16.90
3	−17.35	−17.58	−17.71	−17.81
4	−12.36	−19.06	−16.95	−17.99
Delta	7.57	3.11	0.76	1.46
Rank	1	2	4	3

Table 4
Means for WR.

Level	Wt. % SiC	'P' (N)	'V' (m/s)	'D' (m)
1	10.231	6.715	7.502	6.997
2	9.546	7.175	7.605	7.645
3	7.401	8.041	8.306	8.108
4	4.226	9.472	7.992	8.654
Delta	6.005	2.757	0.804	1.657
Rank	1	2	4	3

Table 5
S/N ratios for COF.

Level	Wt.% of SiC	'P' (N)	'V' (m/s)	'D' (m)
1	4.890	7.545	6.011	5.675
2	5.850	6.719	5.950	5.875
3	5.621	5.311	5.989	5.971
4	7.577	4.363	5.988	6.417
Delta	2.687	3.183	0.061	0.742
Rank	2	1	4	3

Table 6
Means for COF.

Level	Wt.% of SiC	'P' (N)	'V' (m/s)	'D' (m)
1	0.5725	0.4225	0.5025	0.5300
2	0.5175	0.4650	0.5125	0.5200
3	0.5300	0.5475	0.5125	0.5075
4	0.4225	0.6075	0.5150	0.4850
Delta	0.1500	0.1850	0.0125	0.0450
Rank	2	1	4	3

where V = Velocity (m/min), D = diameter (mm) and N = Speed (rpm).

3. Results and discussions

3.1. Characterization studies of powder mixture and sintered composites

Fig. 4(a–d) shows the milled Mg/3Al/SiC powders taken by using SEM. SiC particles are evenly dispersed in the Mg/3Al alloy. In all composite mixtures, SiC is not agglomerated and this is because of the superior milling process. The proportion of SiC content is more in Fig. 4(c) and (d) indicating a greater volume of SiC. The undeviating spreading of SiC particles is important one, since it affects the property of the composites.

SEM images of sintered Mg/3Al based composites are depicted in Fig. 5(a–e). Each image displays the SiC particle distribution uniformly in the grain boundary of the Mg/3Al matrix. According to the results obtained for the SEM analysis, it is clear that, all the samples show excellent bonding between SiC particles and Mg matrix. For the higher proportion of SiC in the sample, there is no agglomeration is observed at it is shown in Fig. 5(c). Due to appropriate ball milling of Mg, Al and SiC, the even spreading is attained. The uniform distribution of SiC particle is important to achieve the good mechanical and wear properties [8]. The proper bonding was achieved due to the suitable sintering time and temperature and the argon atmosphere [10]. The XRD pattern of Mg/3Al/SiC composite milled powders, sintered samples and hardness of the sintered composite were reported in our previous publication [44].

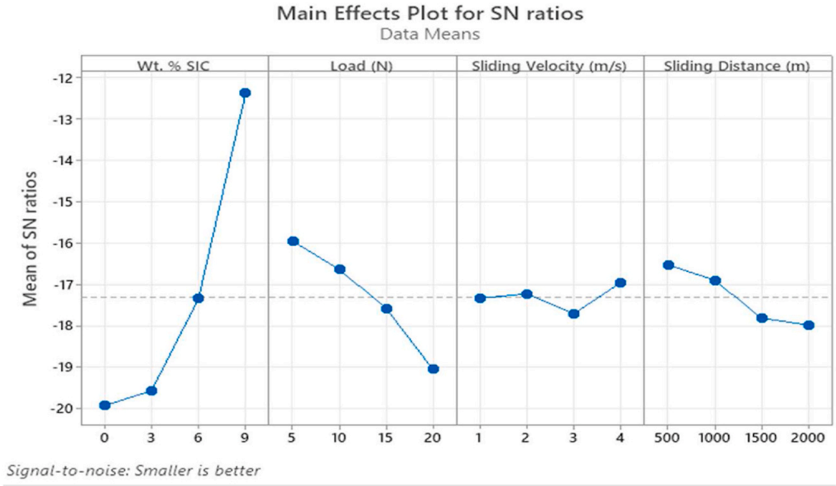

Fig. 6. SN ratio plot of WR.

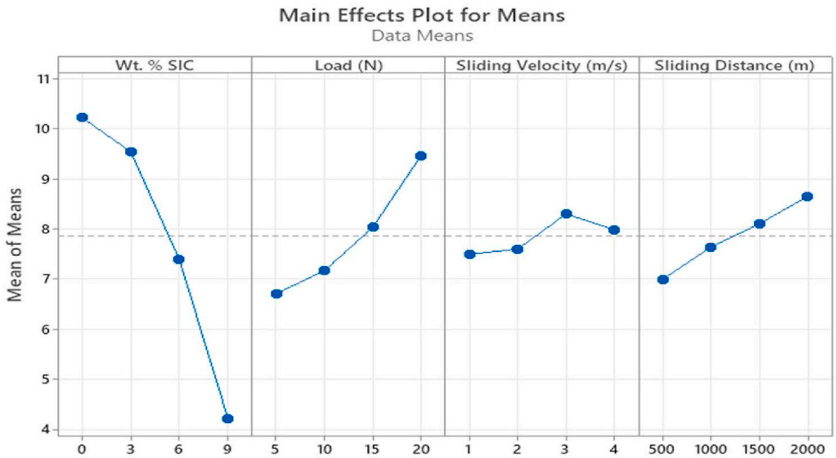

Fig. 7. Mean plot of WR.

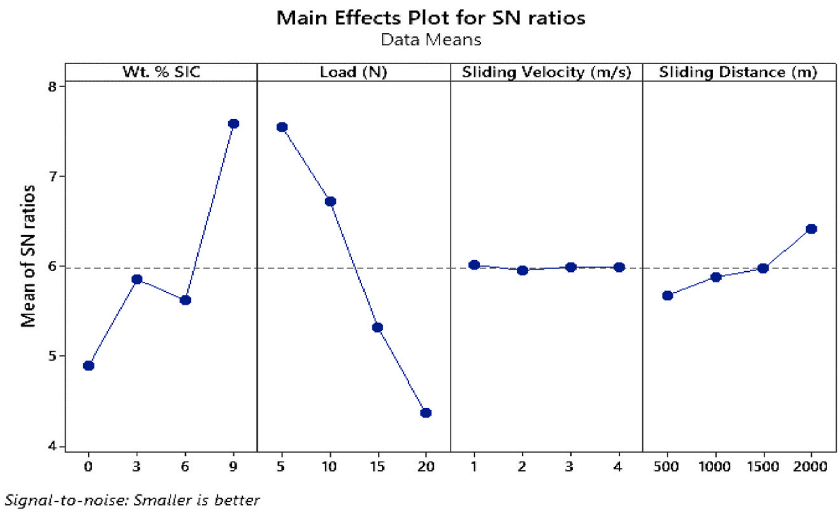

Fig. 8. S/N ratio plot of COF.

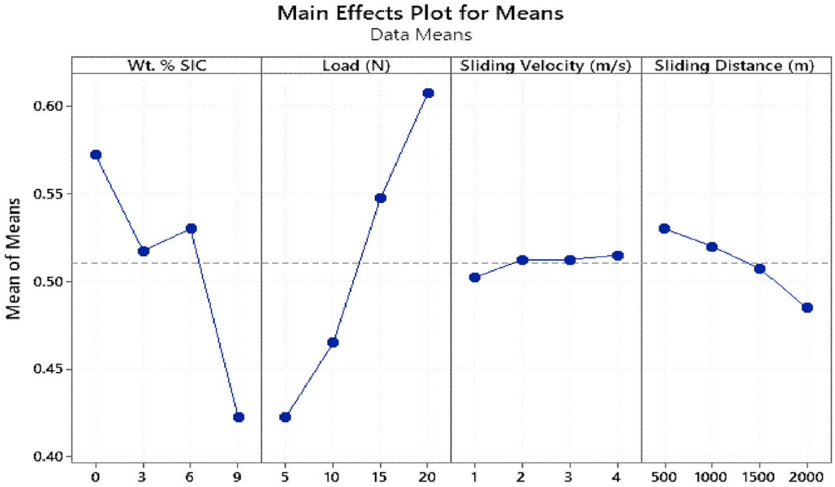

Fig. 9. Mean plot of COF.

3.2. *Taguchi analysis*

3.2.1. *S/N ratio of analysis*

Tables 3–6 shows the S/N ratio and Mean values for the WR and COF. Fig. 6 displays S/N ratio plot of WR. Fig. 7 displays the mean plot for the WR. To achieve the best WR, reinforcement levels of ($A_4B_1C_1D_1$) were found to be optimal at Level IV (9 wt %), 'P' at Level I (5 N), 'V' at Level I (1 m/s) and 'D' at Level I (500 m).

Fig. 8 shows S/N ratio plot of COF. Fig. 9 shows the mean plot for the COF. Based on the results of the investigation, it was evident that the parameters that would achieve the optimum COF were ($A_4B_1C_1D_4$), which means the level of reinforcement at Level I (9 wt %), 'P' at Level I (5 N), 'V' at Level I (1 m/s) and 'D' at Level IV (2000 m). The WR of reinforced alloy is dependent on the applied load. The applied load was deemed to be a significant influence on WR. As the WR changes with the applied load, Archard's law, which explains that the amount of material removed corresponds to the normal pressure or load between surfaces contacting one another, appears to be honoured here [17,21,22]. The WR increases as applied load increases, with composites showing a lower WR than alloy reinforced with Mg/3Al/SiC. A reduction in wear coefficients and volumetric losses with the introduction of metal matrix and reinforcements is likely due to the occurrence of particles in the Mg/3Al matrix. According to the results, this may have resulted from the Mg/3Al particles reducing the rate of material removal coincident with increased hardness of the composites. WR is low at lower loads due to the surface interacting pressure being lower, which is also the result of the existence of SiC particles. However, for reinforced alloys, material removal rates are higher as surface debris clings to them and in turn removes more material due to high pressures at their interfaces [17,22,23]. Many researchers reported that, the reinforcement wt. % is having more impact on WR than the applied load. Suleyman et al. reported that, addition of eggshell content (2.5, 5 and 10 wt %) improved the wear resistance of Mg matrix [38]. Stalin et al. manufactured Si_3N_4 reinforced Al composites observed the low WR (0.002 mm^3) when the reinforcement percentage is high [39]. Kaushik et al. investigated the SiC and Gr reinforced Al6082 hybrid composites and reported that, hybrid composites showed excellent wear resistance [40]. Alipour et al. reported that, the increase in GNP % in AA7068 matrix decreases the wear loss [41]. From the previous literatures it is evident that, the addition of hard reinforcements like SiC and Silicon nitride influenced the WR of the metal matrix composites fabricated by various routes [42,43].

3.2.2. *Contour plot analysis*

Fig. 10(a–f) displays the contour plot for WR. From Fig. 10(a), we could see the plot of WR as a function of 'P' and the weight % of SiC. From these plots, the decrease in WR can be perceived with an increase in SiC weight % in the right corner. The lowest 'WR' was observed for the 9 wt % of SiC as seen in the plot 10 (a). This is due to the incorporation of hard SiC in the soft matrix. Regarding the 'P' and 'D', Fig. 10(a) &(c) follow the same trend. A dotted red line on Fig. 10(b) illustrates how adding reinforcement increases the WR, as seen from its interaction with SiC weight % and 'D'. The high WR was observed for the highest value of 'D' 2000 m as seen in the plot 10 (b). The increase in 'D' increases the 'WR' due to the continually applied load, however the WR decreases due to presence of hard SiC particles in the samples. In Fig. 11(a–f), the COF is plotted for 'P' versus weight percent SiC; 'P' versus 'D' and wt.% of SiC versus 'D'. During the wear testing of composite materials, the COF increase with increasing load. The above factors contribute to the increased wear resistance of the proposed materials, which are hard and have an increased SiC content in the matrix alloy, as well as being wear resistant [21].

WR increase along with sliding velocity. High sliding velocity also results in matrix softening, leading to increased material removal and heavy deformation. Likewise, layers that develop on the surface of pins peel off, which leads to the loss of further material from reinforced alloy specimens. The WR of composites is lower because of the presence of SiC particles, which provide the composite matrix with properties such as hardness. The hardness of composites increases their wear resistance and seizure resistance [20,21].

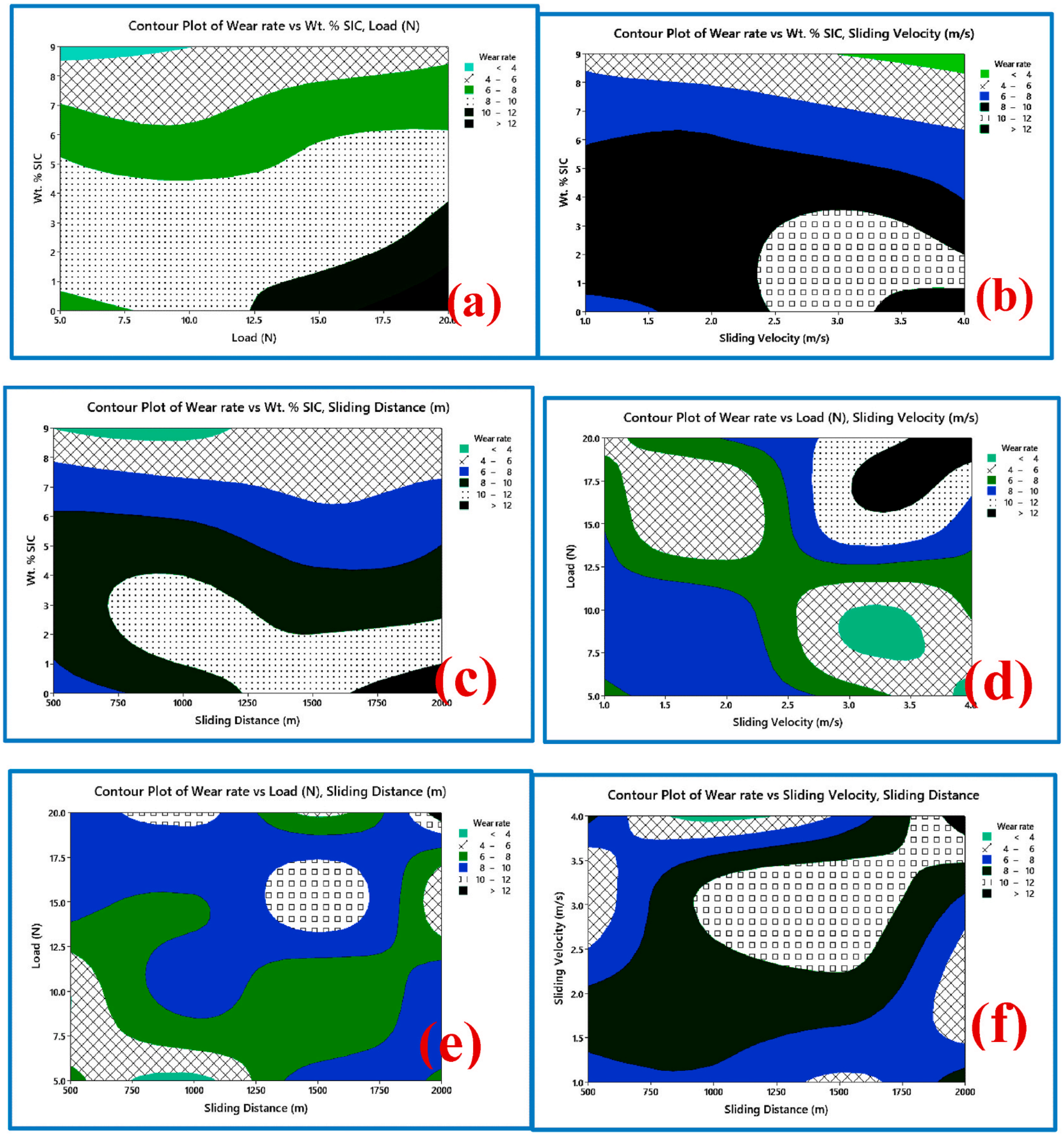

Fig. 10. (a–f) Contour plots for wear rate.

Mg/3Al/SiC composite offer superior wear resistance when the surfaces slide together, the protrusions of the reinforcements that are in contact become blunted and smoothed out. With an increase in "D", the reinforcement particles are smoothed, resulting in the formation of a wear resisting layer that lowers wear. As the "D" is increased, alloys show a greater WR. It is because the pin becomes debilitated, resulting in greater material removal. Therefore, composites perform better at higher distances than alloys, since they have improved properties that increase their hardness. Also, the SiC layer reduced the WR of the composite matrix by serving as an resisting layer between the in-contact surfaces [21–23].

3.2.3. Interaction plot analysis

Interaction plot in Fig. 12 illustrates the impact of controlling parameters on performance characteristics and showing the minimum 'WR' when the reinforcement level is high (9 wt % SiC) and low load. Based on the interaction plot of 'WR' and S/N ratios, it becomes evident that 'WR' depends on the amount of SiC and the load [21]. The domination of SiC wt. % on the 'WR' is clearly seen form the interaction plot (Fig. 12) while interacting the other parameters. The reason is that the hard SiC particles act like wear resisting agent in the matrix materials. Next to SiC wt.%, the interaction of 'P' is higher when compare with the other parameters studied in this work. This is due to the fact that, the 'P' create deformation on the samples. Fig. 13 shows the interaction plot for COF. Similar for the COF, the most influencing factors are combination of load and wt. % of SiC. From the interaction plot it is concluded that, the most influencing combination parameters for both the WR and COF are "P" and "wt. % SiC".

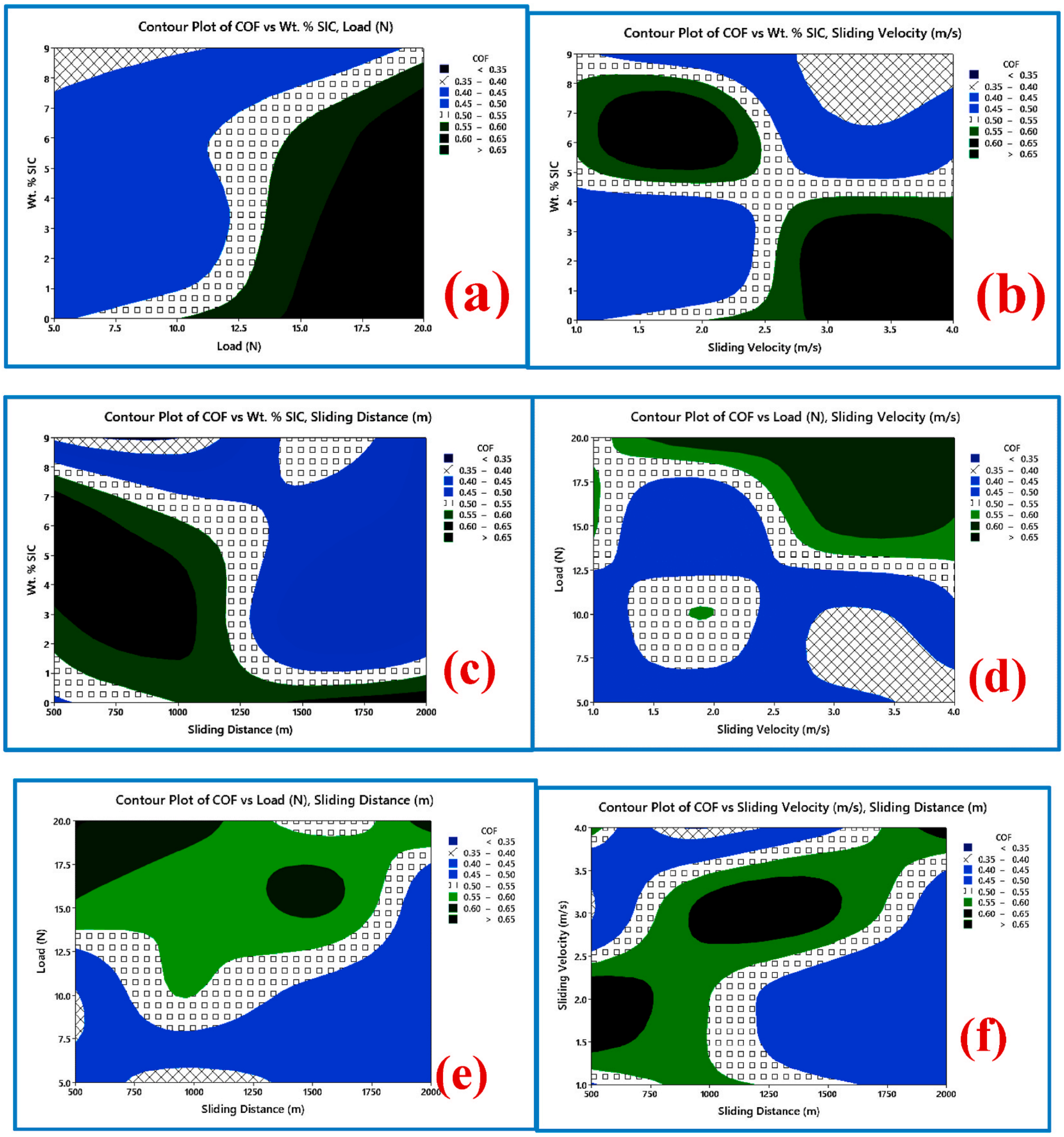

Fig. 11. (a–f) Contour plot for COF.

3.2.4. Analysis of variance

ANOVA was used to study the influence of parameters, such as weight% SiC, 'P', 'V', and 'D' to WR and COF. Table 7 shows ANOVA for WR. According to the F value, 'P', as seen reinforcement and "D", is the most dominant factor. Analysis of variance for COF is provided in Table 8. From the table, it is clear that the 'P' has the highest impact, followed by the content of SiC, the 'D' and the 'V' [17]. Equations (3) and (4) shows the regression equation for WR and COF. Fig. 14 shows the Probability plot of WR and Fig. 15 shows the Probability plot of COF with 95% confidence interval. It ensures the conducted experiments were within the error limit.

3.3. Worn surface analysis

Fig. 16(a–h) displays the surface of the Mg/3Al and Mg/3Al/SiC composites after wear. Fig. 16(a) & (b) displays the surface of Mg/3Al specimen after wear test. The adhesive wear has been observed for the matrix sample. The plastic deformation is realized in the surface due to the load applied on the pin (wear sample). Also fine grooves and scratches are observed in the surface of the sample. Fig. 16(c) & (d) displays the surface of the Mg/3Al/3SiC composites. The wear patterns are clearly seen in the surface of the sample after wear testing. The distributions of the SiC particles are evident in the surfaces which resist wear of the composites. Fig. 16(e) & (f) shows the surface of the Mg/3Al/6SiC composites. The small grooves and less scratch are observed in the surface. This is due to the reinforced surface having higher surface hardness, which makes more resistant to deformation. The surface of the Mg/3Al/9SiC composites is shown in Fig. 16(g) & (h). The abrasive wear mechanism is apparently observed for the samples. During the wear test, the

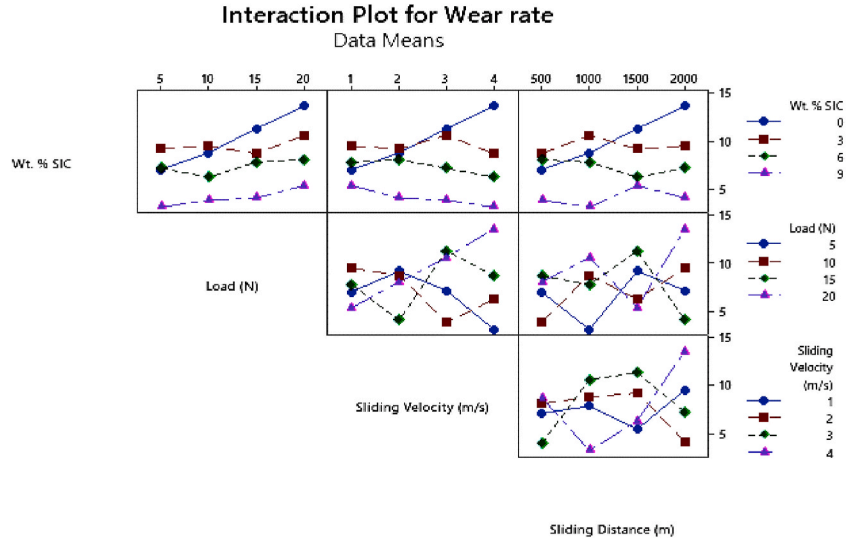

Fig. 12. Interaction plot for WR.

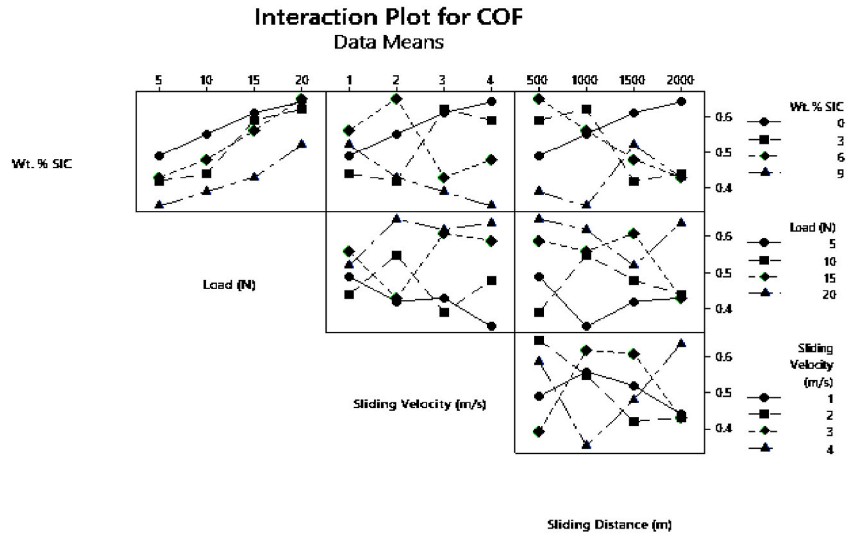

Fig. 13. Interaction plot for COF.

Table 7
ANOVA for WR.

Source	DF	Adj SS	Adj MS	F-Value	P-Value
Wt. % SiC	3	87.524	29.1745	15.49	0.025
'P' (N)	3	17.644	5.8814	3.12	0.187
'V' (m/s)	3	1.634	0.5448	0.29	0.832
'D' (m)	3	5.930	1.9768	1.05	0.485
Error	3	5.649	1.8830		
Total	15	118.382			

Table 8
ANOVA for COF.

$$WR\ X\ 10^{-3}\left(\frac{mm^3}{m}\right) = 7.851 + 2.380A_1 + 1.695A_2 - 0.450A_3 - 3.625A_4 - 1.136B_1 - 0.676B_2 + 0.190\ B_3 + 1.621B_4 - 0.349\ C_1 - 0.246C_2 + 0.454C_3 + 0.140\ C_4 - 0.854D_1 - 0.206\ D_2 + 0.257D_3 + 0.803D_4 \quad (3)$$

$$COF = 0.51062 + 0.06188A_1 + 0.00687A_2 + 0.01937\ A_3 - 0.08813A_4 - 0.08813B_1 - 0.04562B_2 + 0.03688B_3 + 0.09688B_4 - 0.00813\ C_1 + 0.00188\ C_2 + 0.00187C_3 + 0.00437C_4 + 0.01937D_1 + 0.00938D_2 - 0.00313D_3 - 0.02562D_4 \quad (4)$$

Source	DF	Adj SS	Adj MS	F-Value	P-Value
Wt. % SiC	3	0.048069	0.016023	49.62	0.005
‘P’ (N)	3	0.082369	0.027456	85.03	0.002
‘V’ (m/s)	3	0.000369	0.000123	0.38	0.776
‘D’ (m)	3	0.004519	0.001506	4.66	0.119
Error	3	0.000969	0.000323		
Total	15	0.136294			

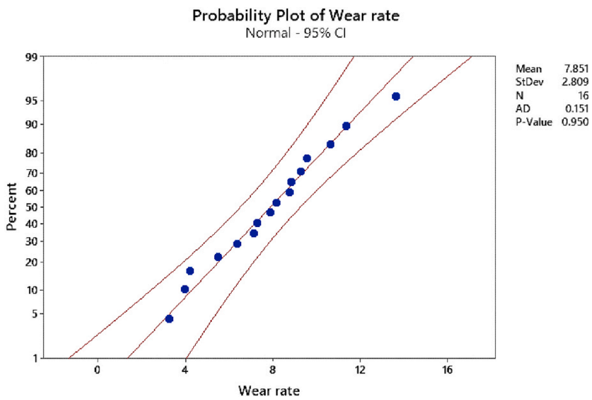

Fig. 14. Probability plot of WR.

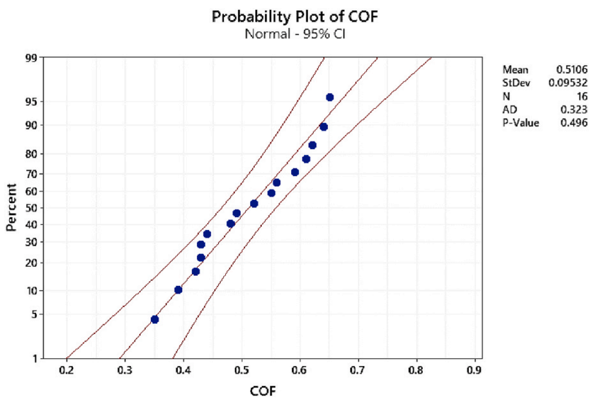

Fig. 15. Probability plot of COF.

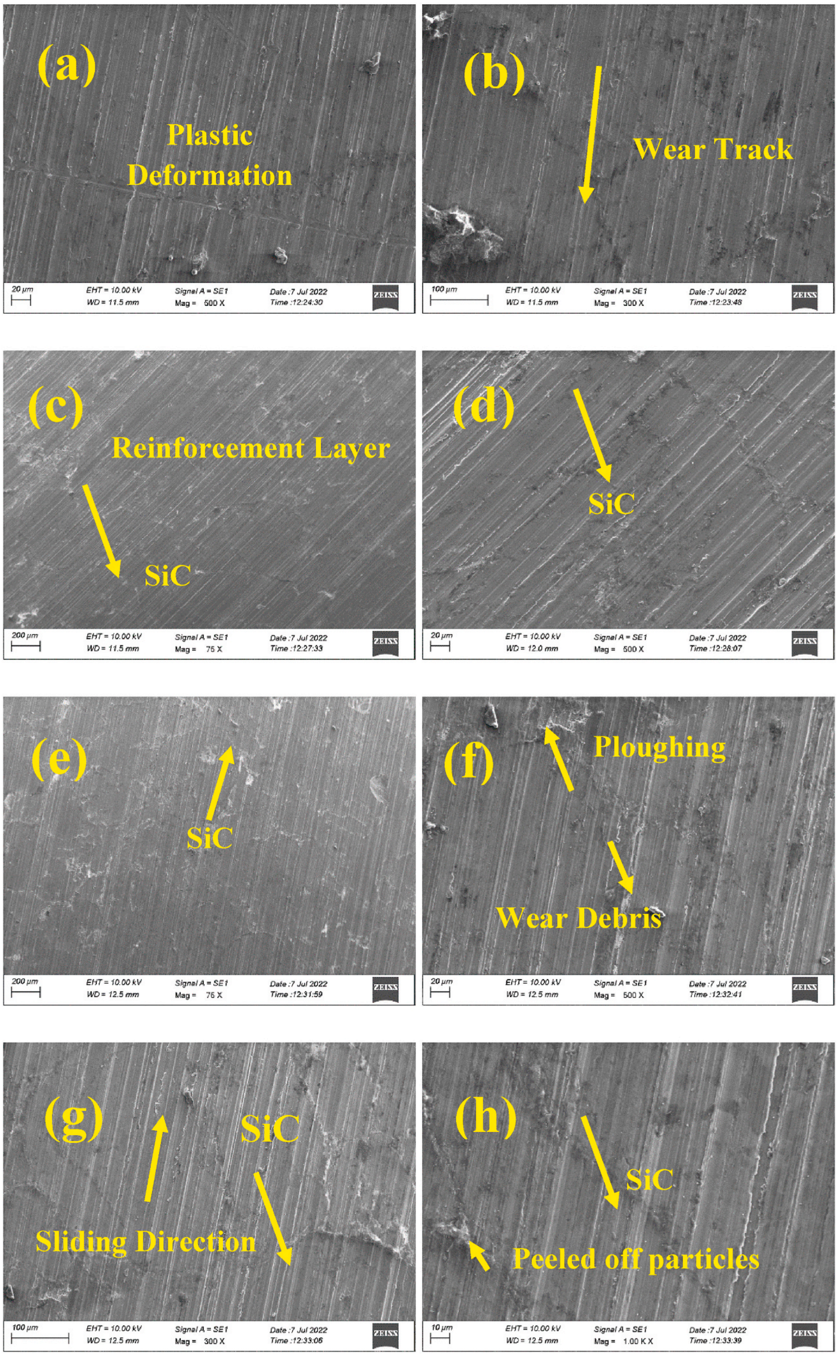

Fig. 16. (a–h) Worn surface analysis of Mg/3Al and its SiC reinforced composites.

reinforced particles stirred and distributed inside the matrix materials properly and less wear was obtained for the reinforced samples [18,21,23].

4. Conclusion

- Mg/3Al alloy based SiC reinforced composite was produced by PM technique and its wear behaviour was completely studied by using SN ratio and ANOVA techniques.
- SEM analysis of Mg/3Al/SiC composite powders shown the uniform distribution of SiC matrix.SEM investigation of sintered Mg/3Al/SiC composite ensured the proper distribution and bonding of SiC in the Mg3Al matrix.

- From the SN ratio analysis, it is found that, wt.% of SiC is the most influencing parameter for the WR of Mg/3Al/SiC sintered composites followed by 'P','D' and 'V'.
- Applied load played major role to affect the COF of the sintered composite during pin on disc testing among the other parameters.
- The effect of wear parameters on the WR and COF were clearly displayed by using contour plots and interaction plot.
- From the ANOVA analysis, based on the F value, the highly influenced parameter for affecting the WR of the sintered Mg/3Al/SiC composite is wt.% of SiC and for COF is applied load.
- Worn surface analysis of the wear samples shown abrasive wear for the composite samples and adhesive wear for the unreinforced samples.

Author contribution statement

S. Jayasathyakawin, M. Ravichandran: Conceived and designed the experiments; Performed the experiments; Analyzed and interpreted the data; Contributed reagents, materials, analysis tools or data; Wrote the paper.

Funding statement

This research did not receive any specific grant from funding agencies in the public, commercial, or not-for-profit sectors.

Data availability statement

No data was used for the research described in the article.

Declaration of interest's statement

The authors declare no conflict of interest.

References

[1] Rajesh Purohit, R.S. Yogesh Dewang, Rana, Dinesh Koli, Shailendra Dwivedi, Fabrication of Mg matrix composites using powder metallurgy process and testing of properties, Mater. Today 5 (2018) 6009–6017.

[2] K.K. Deng, K. Wu, X.J. Wang, Y.W. Wu, X.S. Hu, M.Y. Zheng, W.M. Gan, H.G. Brokmeier, Microstructure evolution and mechanical properties of a particulate reinforced Mg matrix composites forged at elevated temperatures, Mater. Sci. Eng., A 527 (2010) 1630–1635.

[3] Adedotun Adetunla, Anthony Fide-Akwuobi, Benjamin Henry, Adebayo Adeyinka, Adenike Kolawole, A study of degradable orthopedic implant: an insight in magnesium metal matrix composites, Heliyon 8 (9) (2022), e10503.

[4] S. Jayasathyakawin, M. Ravichandran, N. Baskar, C. Anand Chairman, R. Balasundaram, Mg matrix composite for biomedical applications through powder metallurgy–Review, Mater. Today 27 (2020) 736–741.

[5] Tosun Gul, Mehmet Kurt, The porosity, microstructure and hardness of Al-Mg composites reinforced with micro particle SiC/Al_2O_3 produced using powder metallurgy, Compos. B Eng. 174 (2019), 106965.

[6] Janusz Lelito, Pawel L. Zak, Amir A. Shirzadi, A. Lindsay Greer, Witold K. Krajewski, Jozef S. Suchy, Katharina Haberl, Peter Schumacher, Effect of SiC reinforcement particles on the grain density in a Mg-based metal–matrix composite: modelling and experiment, Acta Mater. 60 (2012) 2950–2958.

[7] F. Munarin, P. Petrini, R. Gentilini, R.S. Pillai, S. Dire, M.C. Tanzi, V.M. Sglavo, Micro and nano-hydroxyapatite as active reinforcement for soft biocomposites, Int. J. Biol. Macromol. 72 (2015) 199–209.

[8] Murlidhar Patel, Sushanta Kumar Sahu, Mukesh Kumar Singh, Abrasive wear behavior of SiC particulate reinforced AA5052 metal matrix composite, Mater. Today 33 (2020) 5586–5591.

[9] Vipin Kumar Sharma, Vinod Kumar, Development of rare-earth oxides based hybrid AMCs reinforced with SiC/Al_2O_3: mechanical & metallurgical characterization, J. Mater. Res. Technol. 8 (2019) 1971–1981.

[10] Song-Jeng Huang, AddisuNegash Ali, Effects of heat treatment on the microstructure and microplastic deformation behavior of SiC particles reinforced AZ61 Mg metal matrix composite, Mater. Sci. Eng., A 711 (2018) 670–682.

[11] Huan Yu, Haiping Zhou, Yu Sun, Lili Ren, Zhipeng Wan, Lianxi Hu, Microstructures and mechanical properties of ultrafine-grained Ti/AZ31 Mg matrix composite prepared by powder metallurgy, Adv. Powder Technol. 29 (2018) 3241–3249.

[12] S. Dinesh Kumar, M. Ravichandran, S. Sakthivelu, M. Meignanamoorthy, C. Chanakyan, S.V. Alagarsamy, Mechanical properties of Mg-silicon carbide composite fabricated through powder metallurgy route, Mater. Today 27 (2020) 1137–1141.

[13] Yan Yang, Xin Chu, Xier Luo, Xuemei Xu, Yu Zhang, YiLong Dai, Li Ding, Liangjian Chen, Tao Xiao, Yu Kun, A homogenous microstructural Mg-based matrix model for orthopedic application with generating uniform and smooth corrosion product layer in Ringer's solution: study on biodegradable behavior of Mg-Zn alloys prepared by powder metallurgy as a case, J. Magnes. Alloys. 9 (2021) 225–240.

[14] C. Parswajinan, B. Vijaya Ramnath, M. Vetrivel, A. Riyaz Ahmed, A.S.A. Syed Mohamed Buhari, C. Muthukumaaran, I. Anish Hilary, Design and fabrication of impact die for powder metallurgy, Mater. Today 5 (2018) 329–334.

[15] S. Sharma, Parametric study of abrasive wear of Co–CrC based flame sprayed coatings by response surface methodology, Tribol. Int. 75 (2014) 39–50.

[16] R. Jojith, N. Radhika, Mechanical and tribological properties of LM13/TiO_2/MoS_2 hybrid metal matrix composite synthesized by stir casting, Part, Sci. Technol. 37 (2018) 566–578.

[17] S.V. Alagarsamy, M. Ravichandran, Investigations on tribological behaviour of AA7075-TiO_2 composites under dry sliding conditions, Ind. Lubric. Tribol. 71 (2019) 1064–1071.

[18] S. Dharmalingam, R. Subramanian, M. Kok, Optimization of abrasive wear performance in aluminium hybrid metal matrix composites using Taguchi-grey relational analysis, J. Eng. Tribol. 222 (2014) 749–760.

[19] S.S. Mahapatra, A. Patnaik, A. Satapathy, Taguchi method applied to parametric appraisal of erosion behavior of GF-reinforced polyester composites, Wear 265 (2008) 214–222.

[20] B.A. Kumar, N. Murugan, Metallurgical and mechanical characterization of stir cast AA6061-T6–AlNp composite, Mater. Des. 40 (2012) 52–58.

[21] N. Radhika, R. Raghu, Dry Sliding wear behaviour of aluminium Al–Si12Cu/TiB_2 metal matrix composite using response surface methodology, Tribol. Lett. 59 (2015) 1–9.

[22] N. Radhika, R. Raghu, Evaluation of dry sliding wear characteristics of LM13 Al/B_4C composites, Tribol. Ind. 37 (2015) 20–28.

[23] N. Radhika, R. Raghu, Prediction of mechanical properties and modeling on sliding wear behavior of LM25/TiC composite using response surface methodology, Part. Sci. Technol. 36 (2018) 1–8.
[24] N. Altinkok, I. Ozsert, F. Findik, Dry sliding wear behavior of Al_2O_3/SiC particle reinforced aluminium based MMCs fabricated by stir casting method, Acta Phys. Pol., A 124 (2013) 11–19.
[25] P. Ravindran, K. Manisekar, P. Narayanasamy, N. Selvakumar, R. Narayanasamy, Application of factorial techniques to study the wear of Al hybrid composites with graphite addition, Mater. Des. 39 (2012) 42–54.
[26] S. Suresha, B.K. Sridhara, Effect of addition of graphite particulates on the wear behaviour in aluminium– silicon carbide– graphite composites, Mater. Des. 31 (2010) 1804–1812.
[27] V.R. Rao, N. Ramanaiah, M.M.M. Sarcar, Mechanical and tribological properties of AA7075–TiC metal matrix composites under heat treated (T6) and cast conditions, J. Mater. Res. Technol. 5 (2016) 377–383.
[28] S. Baskaran, V. Anandakrishnan, M. Duraiselvam, Investigations on dry sliding wear behavior of in situ casted AA7075–TiC metal matrix composites by using Taguchi technique, Mater. Des. 60 (2014) 184–192.
[29] S. Dhanalakshmi, N. Mohanasundararaju, P.G. Venkatakrishnan, V. Karthik, Optimization of friction and wear behaviour of Al7075-Al_2O_3-B_4C metal matrix composites using Taguchi method, Mater. Sci. Eng. 314 (2018) 1–9.
[30] S. Garcia-Rodriguez, B. Torres, A. Maroto, A.J. Lopez, E. Otero, J. Rams, Dry sliding wear behavior of globular AZ91 magnesium alloy and AZ91/SiCp composites, Wear 390–391 (2017) 1–10.
[31] Yong Hu, Li Rao, Effect of particulate reinforcement on wear behavior of magnesium matrix composites, Trans. Nonferrous Metals Soc. China 22 (2012) 2659–2664.
[32] Moslem Tayyebi, Morteza Alizadeh, Thermal and wear properties of Al/Cu functionally graded metal matrix composite produced by severe plastic deformation method, J. Manuf. Process. 85 (2023) 515–526.
[33] Pham Van Trinh, Junho Lee, Byungchul Kang, Phan Ngoc Minh, Doan Dinh Phuong, Soon Hyung Hong, Diam Relat Mater 124, 2022, 108952.
[34] P. Dinesh Babu, B. Prasanna kumar, P. Marimuthu, R.K. Mishra, T. Ram Prabhu, Microstructure, wear and mechanical properties of plasma sprayed TiO_2 coating on Al–SiC metal matrix composite, Arch. Civ. Mech. Eng. 19 (2019) 756–767.
[35] Junliu Ye, Xianhua Chen, Huan Luo, Jie Zhao, Jianbo Li, Jun Tan, Hong Yang, Bo Feng, Kaihong Zheng, Fusheng Pan, Microstructure, mechanical properties and wear resistance of Ti particles reinforced AZ31 magnesium matrix composites, J. Magnes. Alloy. 10 (2022) 2266–2279.
[36] Jatinder Kumar, Dilbag Singh, Nirmal S. Kalsi, Shubham Sharma, Catalin I. Pruncu, Danil Yu Pimenov, Kalagadda Venkateswara Rao, Wojciech Kaplonek, Comparative study on the mechanical, tribological, morphological and structural properties of vortex casting processed, Al–SiC–Cr hybrid metal matrix composites for high strength wear-resistant applications: fabrication and characterizations, J. Mater. Res. Technol. 9 (2020) 13607–13615.
[37] Alizadeh Ali, Khayami Ali, Mostafa Karamouz, Mohsen Hajizamani, Mechanical properties and wear behavior of Al5083 matrix composites reinforced with high amounts of SiC particles fabricated by combined stir casting and squeeze casting; A comparative study, Ceram. Int. 48 (2022) 179–189.
[38] Demirdal Suleyman, Fatih Aydin, The influence of low-cost eggshell on the wear and electrochemical corrosion behaviour of novel pure Mg matrix composites, Mater. Chem. Phys. 277 (2022), 125520.
[39] B. Stalin, P.R. Kumar, M. Ravichandran, M.S. Kumar, M. Meignanamoorthy, Optimization of wear parameters using Taguchi grey relational analysis and ANN-TLBO algorithm for silicon nitride filled AA6063 matrix composites, Mater. Res. Express 6 (10) (2019), 106590.
[40] N.C. Kaushik, R.N. Rao, The effect of wear parameters and heat treatment on two body abrasive wear of Al–SiC–Gr hybrid composites, Tribol. Int. 96 (2016) 184–190.
[41] M. Alipour, R. Eslami-Farsani, Synthesis and characterization of graphene nanoplatelets reinforced AA7068 matrix nanocomposites produced by liquid metallurgy route, Mater. Sci. Eng., A 706 (2017) 71–82.
[42] N. Miloradovic, R. Vujanac, B. Stojanovic, A. Pavlovic, Dry sliding wear behaviour of ZA27/SiC/Gr hybrid composites with Taguchi optimization, Compos. Struct. 264 (2021), 113658.
[43] Ashish Kumar, Ravindra Singh Rana, Rajesh Purohit, Anurag Namdev, Kuldeep K. Saxena, Optimization of dry sliding wear behavior of Si_3N_4 and Gr reinforced Al–Zn–Mg–Cu composites using taguchi method, J. Mater. Res. Technol. 19 (2022) 4793–4803.
[44] S. Jayasathyakawin, M. Ravichandran, Experimental investigations on effect of silicon carbide on microstructure and mechanical properties in Mg-3 wt% Al alloy matrix using powder metallurgy, Silicon 14 (2022) 9163–9173.